

Supramolecular copper(II) complexes of novel Schiff bases derived from β -amino acid and salicylaldehyde: Syntheses, crystal structure, and magnetic property

Ya-jin Yan, Fei Yin, Jing Chen, Hang-Li Zhang, Bian-Ling Yan, Yin-Zhi Jiang, Yang Zou*

Chemistry Department, Zhejiang Sci-Tech University, 310018 Hangzhou, PR China

ARTICLE INFO

Article history:

Received 13 July 2013

Received in revised form 19 December 2013

Accepted 8 January 2014

Available online 16 January 2014

Keywords:

Copper complex

β -Amino acid

Schiff-base

Self-assembly

Magnetic

ABSTRACT

Two new ternary mixed-ligand complexes $[\text{Cu}_2(\text{L}^1)_2(\text{bipy})(\text{EtOH})_2]$ (**1**) ($\text{H}_2\text{L}^1 = \beta$ -phenylal-anine, $\text{N}-[1-(2\text{-hydroxyphenyl})\text{propylidene}]$, $\text{bipy} = 4,4'$ -bipyridine, $\text{EtOH} = \text{ethanol}$) and $[\text{CuL}^2(\text{imi})]$ (**2**) ($\text{H}_2\text{L}^2 = \beta$ -(2-chlorophenyl)alanine, $\text{N}-[1-(2\text{-hydroxyphenyl})\text{propylidene}]$, $\text{imi} = \text{imidazole}$) have been synthesized and characterized by X-ray diffraction. In **1**, the coordination geometry around the copper is square-pyramidal. The Schiff base ligand L^1 coordinates to the $\text{Cu}(\text{II})$ ion in a tridentate mode, while the bipyridine ligand coordinates in bidentate bridging mode linking two adjacent $\text{Cu}(\text{II})$ ions. The binuclear unit are further linked by hydrogen bond to form a 2D wave-like supramolecular architecture. In **2**, the coordination geometry around the copper is distorted square-planar. In the solid state, the imidazole ring is hydrogen-bonded to the carboxyl group, thus linked the two adjacent $\text{CuL}^2(\text{imi})$ units together with a $\text{Cu}-\text{Cu}$ distance of 3.515 Å. Magnetic behaviors of complex **1** and **2** exhibit antiferromagnetic interactions within the $\text{Cu}(\text{II})$ dimer fitted by the spin Hamiltonian $H = -JS_1S_2$.

© 2014 Elsevier B.V. All rights reserved.

1. Introduction

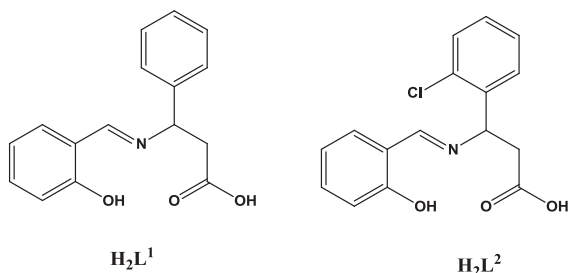
The design and construction of transition metal supramolecular complexes with amino-acid-based Schiff bases have attracted great interest, not only because of their potential applications in magnetism, asymmetric catalysis, luminescent probes, and biological functional materials, but also for the tremendous structural diversity of these complexes [1,2]. In general, coordination supramolecular complexes can be assembled through two major chemical processes: coordinate chemistry and supramolecular chemistry (e.g. strong hydrogen bonds, C–H hydrogen bonds, π – π stacking interactions, etc.) [3]. The majority of amino-acid-based Schiff bases applied so far are derived from a condensation reaction of salicylaldehyde (or its derivatives) with amino acids, which contain a phenoxyl oxygen atom, an imine nitrogen atom and carboxylate group. Based on the coordination modes, the coordination of these ONO tridentate ligands with metal ions usually generate the following types of complexes: (a) mononuclear unit with the carboxylate group, using a monodentate mode [4]; (b) multinuclear complexes with metal centers bridged by phenoxyl O atom, syn-anti carboxylate anion, or a functional group in the side chain of the L ligand [5]; (c) 1D helical/zigzag chains via syn-anti, anti-anti,

or monodentate carboxylate bridges [6]; and (d) a 2D network with metal ions linked by phenoxyl O atom and syn-anti carboxylate group [7]. Meanwhile, amino acids are naturally potential candidates for hydrogen-bonded supramolecular networks because the amino groups and carboxylate groups of amino acids are excellent hydrogen bond donors and acceptors [8]. Numerous studies have been directed at supramolecular assembly of amino acid Schiff bases (or reduced amino acid Schiff bases), they are mainly devoted to simple amino acids such as glycine [9–13], valine [13,14], phenylalanine [13,15–17], etc. Comparatively, studies involving functional β -amino acids are significantly less explored. β -Amino acid Schiff base ligand can form two 6-membered chelate rings when coordinates with metal, while α -amino acid Schiff base ligand usually forms one 6-membered and one 5-membered chelate ring. The introduction of the β -amino acid in the Schiff base ligand should not be expected to augment their metal binding capabilities but may enhance the tendency of the formation of stable secondary structures [18].

On the other hand, copper is an element with relevant oxidation states in the first-row transition metal, and its amino Schiff base complexes with imidazole, pyrazole, pyridine, Phenanthroline (bipyridine) etc. as coligands have been received much attention. The products have been investigated by ESR and their magnetism, catalytic and redox activities have also been tested [19]. Meanwhile, 4,4'-bipyridine generally coordinates in bridging fashion,

* Corresponding author. Tel.: +86 571 86843230.

E-mail address: zouyang@zstu.edu.cn (Y. Zou).



Scheme 1. Schematic representation of ligands H_2L^1 and H_2L^2 .

which usually gives rise to extended metal-ligand structures with linear 4,4'-bipyridine acting as a spacer.

In this paper, we report the synthesis of new ligand H_2L^2 (β -(2-chlorophenyl)alanine, N-[1-(2-hydroxyphenyl)propylidene] **Scheme 1**) and characterization of two Cu(II) complexes of β -amino-acid-based Schiff base: $[Cu_2(L^1)_2(bipy)(EtOH)_2]$ **1** and $[CuL^2(imi)]$ **2** ($bipy$ = 4,4'-bipyridine, $EtOH$ = ethanol and imi = imidazole).

2. Experimental

2.1. Materials and methods

All chemicals were of reagent grade and were used as supplied by commercial sources. FT-IR spectra were measured from KBr pellets using a Nicolet FT-IR 400 system in the range of 4000–400 cm^{-1} . The 1H NMR spectra was recorded on an Avance AV 400 MHz Digital FT-NMR Spectrometer at room temperature in D_2O . Elemental microanalyses (EA) were performed on a Perkin-Elmer CHN-2400 analyzer. PXRD data were recorded using a Bruker D8 system with Cu $K\alpha$ radiation (λ = 0.15405 nm). Thermal gravimetric analysis (TGA) were performed using a Perkin Elmer series 7 instrument in N_2 flowing with a heating rate of 10 $^{\circ}C\ min^{-1}$. The temperature-dependent magnetic susceptibility of **1** was measured with crystalline powder samples on a Quantum Design MPMS XL-7 Squid magnetometer in a magnetic field of 1000 Oe under the temperature range 2–300 K. The diamagnetic contributions of the samples were corrected by using Pascal's constants. Single crystal X-ray diffraction data was collected on a Bruker SMART APEX CCD-based X-ray diffractometer equipped with a normal focus Mo-target X-ray tube (λ) 0.71073 Å). Details of structure analysis are described below.

2.2. Synthesis

2.2.1. Ligand H_2L^1 and H_2L^2 synthesis

H_2L^1 : The ligand H_2L^1 was prepared by condensing DL- β -phenylalanine and salicylaldehyde according to the reported procedure [20]. Yield 87%. (Anal. Calc. for $C_{16}H_{14}O_3N$: C, 69.8; H, 5.1; N, 5.1. Found: C, 69.5; H, 5.2; N, 5.0%); IR (KBr pellet, cm^{-1}): 3369 (br), 1655 (vs), 1601 (s), 1528 (s), 1450 (m), 1423 (s), 1353 (w), 1226 (w), 1175 (w), 892 (w), 775 (m), 661 (w); UV-Vis [5 mM, nm (intensity)]: 202 (2.78), 211 (2.16), 366 (0.325).

H_2L^2 : Ligand H_2L^2 was prepared as for H_2L^1 : DL- β -(2-chlorophenyl)alanine (2.01 g, 10 mmol) was dissolved in refluxing methanol (60 mL) containing $LiOH \cdot H_2O$ (0.42 g, 10 mmol). After cooling to room temperature, a solution of salicylaldehyde (1.22 g, 10 mmol) in methanol (20 mL) was added slowly with stirring. After stirring at room temperature for 1 h, the volume was reduced to ca. 10 mL in vacuum. Anhydrous ether 200 mL was added to precipitate the product. The product was isolated as an off-white solid. Yield 2.78 g, 90%. (Anal. Calc. for $C_{16}H_{13}O_3NCl$: C, 55.7; H, 3.8; N, 4.1. Found: C, 54.3; H, 4.0; N, 4.0%. The percentage of carbon

measured is off 1.4% from the calcd one, which may be due to the sample absorbed small amount of water from air.); 1H NMR in D_2O (ppm), 3.06 (2H, d), 4.98 (1H, t), 7.19–7.25 (2H, m), 7.42–7.51 (3H, m), 7.71 (1H, t), 7.79–7.83 (2H, m), 8.77 (1H, s); IR (KBr pellet, cm^{-1}): 3421 (br), 1629 (vs), 1600 (s), 1508 (s), 1413 (s), 1384 (s), 1276 (w), 1220 (s), 1053 (w), 835 (m), 758 (m); UV-Vis [5 mM, nm (intensity)]: 200 (1.82), 208 (1.05), 315 (0.325).

2.2.2. $[Cu_2(L^1)_2(bipy)(EtOH)_2]$, (**1**)

To the ethanol solution (150 mL) of H_2L^1 ligand (1.372 g, 5 mmol), $Cu(NO_3)_2 \cdot 3H_2O$ (1.206 g, 5 mmol) was added, then 4,4'-bipyridine (0.782 g, 5 mmol) was added. After stirring at room temperature for 2 h, the solution was filtered. The filtrate was allowed to evaporate slowly at room temperature. After about one week green crystals suitable for X-ray crystal analysis were obtained. Yield 33%. (Anal. Calc. for $C_{46}H_{48}O_8N_4Cu_2$: C, 60.6; H, 5.3; N, 6.1. Found: C, 60.1; H, 5.4; N, 6.1%). IR (KBr pellet, cm^{-1}): 3429 (w), 1672 (s), 1616 (vs), 1531 (m), 1450 (s), 1415 (m), 1371 (m), 1307 (m), 1226 (w), 1156 (m), 1074 (w), 921 (w), 752 (m), 706 (w), 636 (m). UV-Vis [5 mM, nm (intensity)]: 205 (1.82), 216 (1.49), 374 (0.30), 600 (0.05).

2.2.3. $[CuL^2(imi)]$, (**2**)

To the ethanol solution (200 mL) of H_2L^2 ligand (1.545 g, 5 mmol), $Cu(NO_3)_2 \cdot 3H_2O$ (1.210 g, 5 mmol) was added, then imidazole (0.343 g, 5 mmol) was added. After stirring at room temperature for 2 h, the solution was filtered. The filtrate was allowed to evaporate slowly at room temperature. After about one week green crystals suitable for X-ray crystal analysis were obtained. Yield 63%. (Anal. Calc. for $C_{19}H_{16}O_3N_3ClCu$: C, 52.8; H, 3.7; N, 9.7%. Found: C, 52.7; H, 3.7; N, 9.7%). IR (KBr pellet, cm^{-1}): 3427 (w), 1638 (s), 1614 (vs), 1535 (m), 1450 (s), 1401 (m), 1325 (m), 1198 (w), 1148 (m), 1090 (w), 924 (w), 755 (m), 671 (w). UV-Vis [5 mM, nm (intensity)]: 199 (2.72), 212 (1.16), 362 (0.33), 650 (0.11).

2.3. X-ray Crystallography analysis

Intensities of reflections were measured by using graphite monochromatized Mo $K\alpha$ radiation (λ = 0.71073 Å) at 293(2) K. Multi-scan absorption corrections were applied by using SADABS program.[21] The structure was solved by direct methods. The Cu atoms were located from E-maps and the other non-hydrogen atoms were obtained in successive difference Fourier syntheses. The final refinement was performed by full-matrix least-squares methods on F^2 by the SHELXL-97 program package.[22] All non-hydrogen atoms were treated anisotropically. The H atom of O–H was refined with distance restraint of O–H = 0.82 Å and $U_{iso}(H)$ = 1.5 $U_{eq}(O)$. Other H atoms were positioned geometrically and constrained as riding atoms with C–H = 0.93–0.98 Å and N–H = 0.86 Å, $U_{iso}(H)$ = 1.2 $U_{eq}(C,N)$. Crystallographic data and experimental details for structural analysis are summarized in Table 1. Selected bond lengths and angles are listed in Tables 2 and 3.

3. Results and discussion

3.1. Description of the crystal structure of $[Cu_2(L^1)_2(bipy)(EtOH)_2]$, (**1**)

A perspective view of $[Cu_2(L^1)_2(bipy)(EtOH)_2]$ binuclear complex, showing the atomic numbering scheme, is depicted in Fig. 1. In the solid state, the copper coordination geometry can be described as distorted square-pyramidal geometry. Copper forms two 6-membered chelate rings with the tridentate ligand, which is similar to the previously reported complex $[Cu_2(L^1)_2(imi)_2]$ [20]. The ONO donor set of Schiff base ligand $[Cu(1)–N(1) = 1.965(5)$ Å, $Cu(1)–O(1) = 1.909(4)$ Å, $Cu(1)–O(2) = 1.947(4)$ Å] and one nitrogen

Table 1
Crystal structure parameters for the complexes **1** and **2**.

CCDC deposit no.	CCDC-876705	CCDC-936230
Empirical formula	C ₄₆ H ₄₈ O ₈ N ₄ Cu ₂	C ₁₉ H ₁₆ N ₃ O ₃ ClCu
Formula weight	911.98	433.35
T (K)	293	293
Crystal system	monoclinic	triclinic
Space group	P2 ₁ /c	P1
Unit cell dimensions		
a (Å)	13.069(7)	9.197(3)
b (Å)	18.498(9)	9.590(3)
c (Å)	9.184(5)	11.440(4)
α (°)		66.02(1)
β (°)	106.012(7)	86.44(1)
γ (°)		77.15(1)
V/Å ³	2134.1(2)	898.4(5)
Z	2	2
D _c (g cm ⁻³)	1.419	1.602
Absorption coefficient (mm ⁻¹)	1.055	1.390
F(000)	948	442
Crystal size (mm)	0.20 × 0.20 × 0.10	0.15 × 0.10 × 0.10
θ (°)	2.6–25.0	2.0–25.0
Tot., Uniq. Data, R _{int}	10605, 3734, 0.071	4505, 3104, 0.042
Goodness-of-fit (GOF) on F ²	1.06	1.00
Data/restraints/parameters	3734/0/272	3104/0/244
Final R indices [I > 2σ(I)]	R ₁ = 0.0698, wR ₂ = 0.1741	R ₁ = 0.0542, wR ₂ = 0.0850
R indices (all data)	R ₁ = 0.1075, wR ₂ = 0.1997	R ₁ = 0.1181, wR ₂ = 0.0903
Largest difference in peak and hole (e Å ⁻³)	0.66, −0.77	0.48, −0.31

Table 2
Selected bond lengths (Å) and angles (°) for the complex **1**.

Bond lengths (Å)			
Cu(1)–O(1)	1.909(4)	Cu(1)–O(2)	1.947(4)
Cu(1)–N(1)	1.965(5)	Cu(1)–N(2)	2.045(5)
Cu(1)–O(1S)	2.526(5)	N(1)–C(7)	1.298(7)
N(1)–C(8)	1.473(7)		
Bond angles (°)			
O(1)–Cu(1)–O(2)	173.52(18)	O(1)–Cu(1)–N(1)	92.65(17)
O(1)–Cu(1)–N(2)	88.33(17)	O(1)–Cu(1)–O(1S)	89.63(16)
O(2)–Cu(1)–N(1)	93.08(16)	O(2)–Cu(1)–N(2)	87.25(15)
O(2)–Cu(1)–O(1S)	87.33(15)	N(1)–Cu(1)–N(2)	160.8(2)
O(1S)–Cu(1)–N(1)	90.34(19)	O(1S)–Cu(1)–N(2)	108.91(19)

Table 3
Selected bond lengths (Å) and angles (°) for the complex **2**.

Bond lengths (Å)			
Cu(1)–O(1)	1.906(3)	Cu(1)–O(2)	1.933(3)
Cu(1)–N(1)	1.959(4)	Cu(1)–N(2)	1.971(4)
N(1)–C(8)	1.487(6)	N(1)–C(7)	1.300(6)
Bond angles (°)			
O(1)–Cu(1)–O(2)	173.41(16)	O(1)–Cu(1)–N(1)	93.94(17)
O(1)–Cu(1)–N(2)	86.64(17)	O(2)–Cu(1)–N(2)	87.16(17)
O(2)–Cu(1)–N(1)	92.56(17)	N(1)–Cu(1)–N(2)	170.24(18)

atom of 4,4'-bipyridine [Cu(1)–N(2) = 2.045(5) Å] occupy the corners of a square while one oxygen atom from ethanol occupy the apical position [Cu(1)–O(1s) = 2.526(5) Å]. This bond length is similar to those reported in literature [23]. The values 1.473(7) Å for C(8)–N(1) bond shorter than the usual C–N single bond and the double bond C(7)–N(1) length of 1.298(7) Å agree well with the values of Schiff Base type I described by Ueki et al. [24]. The slight distortion in square-pyramidal geometry of Cu(II) can be attributed to the rigidity of the organic ligand and the strong steric effect between the phenyl rings and the oxygen atoms around the metal. The Cu(II) atom ligating at the basal positions is located by 0.18 Å above the least-square plane defined by the basal four ligating atoms. The

O(1)–Cu(1)–O(2) angle of 173.52(18)° is nearly linear. Angular distortions in the square plane are also caused by different bite angles in the 6-membered chelate rings. Thus, the angles O(2)–Cu(1)–N(1) = 93.08(16)° and O(1)–Cu(1)–N(1) = 92.65(17)° are greater than the ideal value of 90°. The two pyridine rings of the 4,4'-bipyridine molecule is coplanar, and 4,4'-bipyridine acts as a bridge ligand linking the two adjacent Cu(II), with the Cu–Cu distance 11.220 Å. Comparatively in [Cu₂(L¹)₂(imi)₂], the carboxylate group of the ligand but not the imidazole, link two copper centers to form the binuclear complex [20].

The hydrogen atom of ethanol (H(1sa)) are involved in hydrogen bond with the carboxylic oxygen (O(3)) of the Schiff-base ligand. The H···O distance is 1.910 Å. As shown in Fig. 2, the binuclear molecular unit is linked with adjacent four units by intermolecular hydrogen bond (O(1s)–H(1sa)···O(3))^{#1} symmetry code #1: x, −y + 1/2, z + 1/2 to formed a two dimensional wave-like structure, which can be simplified as a (4,4) network. The 2D structure is further stabilized by π–π stacking interactions with interplanar distance of 3.5291(3) Å, and the slip angle of 10.671°.

3.2. Description of the crystal structure of [Cu L²(imi)] (**2**)

The racemic [Cu L²(imi)] (**2**) shows a mildly distorted square-planar geometry and also forms two 6-membered chelate rings with the ligand (Fig. 3). Tridentate ONO donor set of L² ligand [Cu(1)–N(1) = 1.959(4) Å, Cu(1)–O(1) = 1.906(3) Å, Cu(1)–O(2) = 1.933(3) Å] and the N(2) [Cu(1)–N(2) = 1.971(4) Å] of imidazole occupy the corners of a square. The values 1.487(6) Å for the C(8)–N(1) bond, short than the usual C–N single bond and 1.300(6) Å for double bond [C(7)–N(1)]. A slight distortion in the square-planar environment of Cu^{II} is indicated by the observed bond angles, which vary from 86.64(17) to 93.94(17)°. The O(1)–Cu(1)–O(3) angle of 173.41(16)° is nearly linear. The phenyl ring [C(1)–C(6)] and the ring of C(1), C(6), C(7), N(1), O(1), Cu(1) chelate ring are almost coplanar with a small dihedral angle of 0.7°. In the solid state, the imidazole ring is hydrogen-bonded to the carboxyl group of the adjacent ligand, thus linked the two CuL²(imi) units together with a Cu–Cu distance of 3.515 Å (Fig. 4). The coordination mode and structure of **2** is similar to that found in previously reported one [25], except that the substituent on the β site of the amino acid is 4-chlorophenyl rather than 2-chlorophenyl.

3.3. Thermogravimetric Analysis (TGA) and Powder X-ray diffraction (PXRD)

The thermal stability of the water clusters was studied by the thermogravimetric (TG) analysis of freshly grown air-dried crystals of **1** (Fig. S1). The first weight loss of 10.6% in the temperature range 90–225 °C corresponds to loss of ethanol molecules (calculated 10.1%). Decomposition of the framework is observed above 295 °C. For **2**, TGA display a one-step weight loss above 270 °C.

The similarity of the powder X-ray diffraction (PXRD) pattern of **1** and **2** together with the simulated PXRD pattern from the single crystal structure, as shown in Fig. S2, suggests the consistency of the powder sample.

3.4. IR spectrum and electronic spectrum

The IR spectrum of complexes **1** and **2** is consistent with the structural data presented in this work.

In the Schiff base, C=N occurs at 1655 cm⁻¹ for ligand H₂L¹ (1629 cm⁻¹ for H₂L²). After complexation with Cu(II), C=N shifts to lower frequencies of 1616 cm⁻¹ for **1** (1614 cm⁻¹ for **2**) indicating coordination of the imine nitrogen to Cu(II). For **1**, the ν_{as}(COO⁻) is assigned to the strong band at 1531 cm⁻¹ whereas the ν_s(COO⁻) is attributed to the 1450 cm⁻¹ band (for **2**: ν_{as}(COO⁻) = 1535 cm⁻¹,

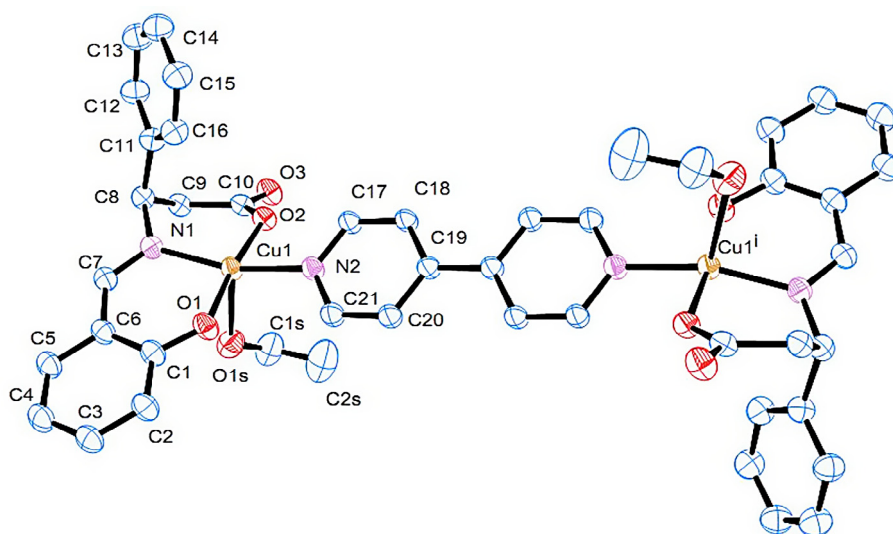


Fig. 1. Molecular structure of the complex **1**. Displacement ellipsoids are drawn at the 30% probability level. Hydrogen atoms are omitted for clarity.

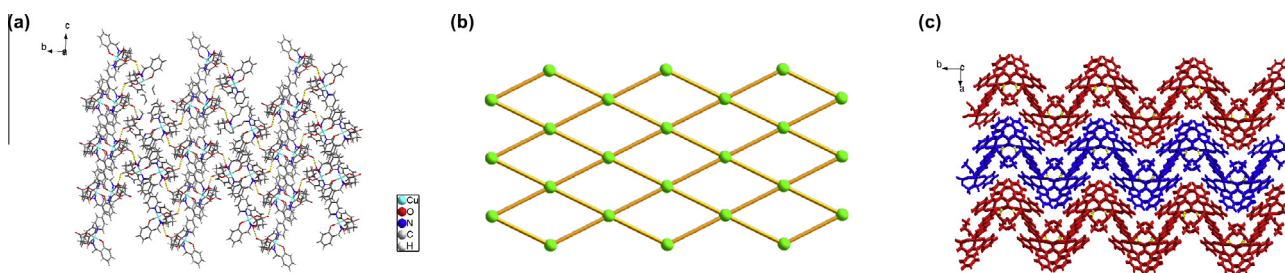


Fig. 2. (a) Hydrogen-bonded 2D framework of **1**, (yellow dash line refer to H-bond); (b) Simplified hydrogen-bonded (4,4) net of **1**, green nodes refer to binuclear molecule unit, yellow sticks refer to H-bond; (c) Hydrogen-bonded wave-like structure of **1** along *b* axis. (For interpretation of the references to colour in this figure legend, the reader is referred to the web version of this article.)

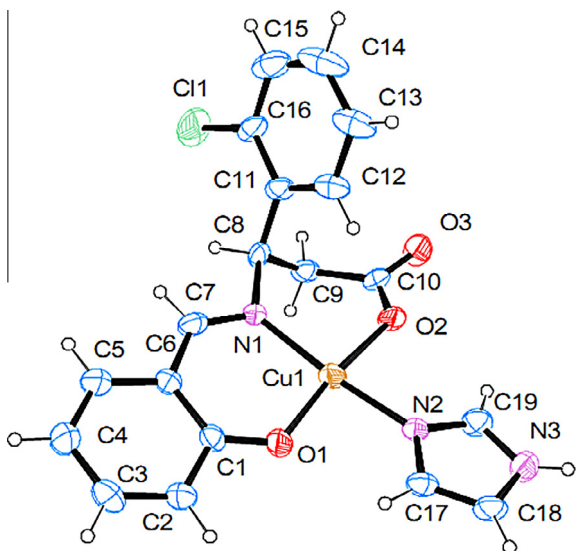


Fig. 3. Molecular structure of the complex **2**. Displacement ellipsoids are drawn at the 30% probability level.

$\nu_s(\text{COO}^-) = 1450 \text{ cm}^{-1}$. An absorption band at 636 cm^{-1} for **1** (671 cm^{-1} for **2**) may be assigned for $\nu(\text{Cu-N})$. The band in the region 1156 cm^{-1} for **1** (1148 cm^{-1} for **2**) may be assigned for $\nu(\text{C-O})$ stretching [26].

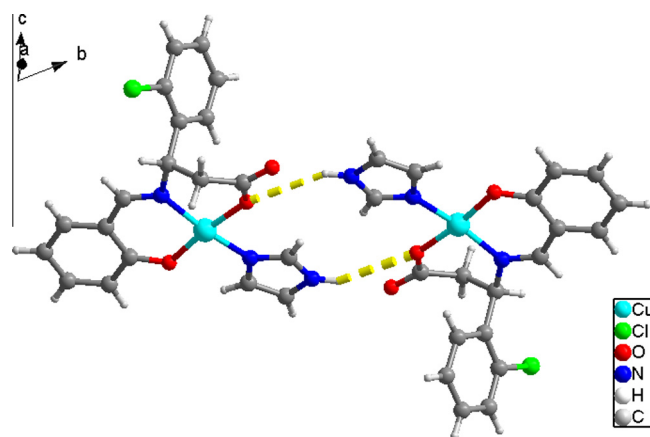


Fig. 4. Structure of complex **2** showing the hydrogen bonding dimeric unit (yellow dashed line refers to hydrogen bond). (For interpretation of the references to colour in this figure legend, the reader is referred to the web version of this article.)

$\pi-\pi^*$ transitions of benzene ring are observed at $\sim 211 \text{ nm}$ for the ligand H_2L^1 (208 nm for H_2L^2) and $\sim 216 \text{ nm}$ for **1** (212 nm for **2**). There is a peak for both the ligands and for the complexes at approximately 200 nm , which may be attributed to the $n \rightarrow \pi^*$ transition of the phenols. The peaks at approximately 370 nm in the spectra of the ligand H_2L^1 (315 nm for H_2L^2) and 374 nm in that of **1** (362 nm for **2**) are assigned to the imine $n-\pi^*$ transitions. The

weak asymmetric broad band at 600 nm observed for **1** and 650 nm, observed for **2**, is assigned to a *d–d* transition.

3.5. Magnetic properties

The magnetic susceptibility of the polycrystalline sample of **1** and **2** were examined within 2–300 K. The results are shown in Figs. 5 and 6 with χ_M and $\chi_M T$ versus *T* plots. At room temperature, the $\chi_M T$ value of the presented complex is $0.856 \text{ cm}^3 \text{ mol}^{-1} \text{ K}$. This value correspond to two isolated copper(II) ions with one unpaired electron with *g* = 2.13. With decreasing temperature, the $\chi_M T$ value remains almost constant until *ca.* 25 K and then it decreases sharply, giving the minimum value of $0.529 \text{ cm}^3 \text{ mol}^{-1} \text{ K}$ at 2 K. The drop in $\chi_M T$ at low-temperatures indicates the presence of a very weak antiferromagnetic coupling between the copper(II) ions. Analysis of the experimental magnetic data was performed by using the Bleaney–Bowers expression,[27] based on the following isotropic Hamiltonian: $H = -J(S_1 S_2)$:

$$\chi_M T = \frac{Ng^2 \beta^2}{k} \frac{2 \exp(J/kT)}{1 + 3 \exp(J/kT)}. \quad (1)$$

The parameters *N*, β and *k* in Eq. (1) have their usual meanings, *J* = Singlet–triplet splitting. Least-square fitting of experimental data leads to the following parameter *J* = $-3.14(5) \text{ cm}^{-1}$ and *g* = $2.13(1)$ for **1** ($R = \sum[(\chi_M T)_{\text{obs}} - (\chi_M T)_{\text{calc}}]^2 / \sum[(\chi_M T)_{\text{obs}}]^2 = 1.7 \times$

10^{-4}) indicating a very weak coupling. This weak magnetic exchange can be understood considering the large Cu–Cu distance (11.22 \AA) [28].

For **2**, the value of $\chi_M T$ is $0.881 \text{ cm}^3 \text{ mol}^{-1} \text{ K}$ at 300 K, which is also close to the value of $0.87 \text{ cm}^3 \text{ mol}^{-1} \text{ K}$ expected for two magnetically independent Cu(II) (*S* = 1/2) centers. It decreases slowly from room temperature to 10 K ($0.788 \text{ cm}^3 \text{ mol}^{-1} \text{ K}$) and then decreases rapidly at a low temperature reaching a value of $0.506 \text{ cm}^3 \text{ mol}^{-1} \text{ K}$ at 2 K. Analysis of the experimental magnetic data was also performed by using Eq. (1). Least-square fitting leads to $g = 2.11(1)$, $J = -0.47(2) \text{ cm}^{-1}$ ($R = \sum[(\chi_M T)_{\text{obs}} - (\chi_M T)_{\text{calc}}]^2 / \sum[(\chi_M T)_{\text{obs}}]^2 = 9.0 \times 10^{-4}$). The negative value of *J* indicates the existence of weak antiferromagnetic coupling interactions in **2**.

4. Conclusions

In conclusion, copper complex with Schiff base ligands containing β -amino acid: $[\text{Cu}_2\text{L}_2(\text{bipy})_2(\text{EtOH})_2]$ **1** and $[\text{CuL}^2(\text{imi})]$ **2** were prepared. In the crystal structure of **1**, each Cu(II) ion is five-coordinated with tridentate chelating Schiff base ligand, ethanol molecule and the 4,4'-bipyridine, which linked two adjacent metal centers to form the binuclear complex. The binuclear unit are further linked by hydrogen bond to construct a 2D wave-like supramolecular architecture. In complex **2**, Cu(II) ion is four-coordinated with a square-planar geometry. The imidazole-carboxyl hydrogen bond linked the two $\text{CuL}^2(\text{imi})$ units together. The variable temperature magnetic susceptibility measurements of **1** and **2** revealed that weak antiferromagnetic coupling interaction exist.

Acknowledgments

This work was financial support by the National Natural Science Foundation of China (No. 20901067), Qianjiang Talent Project (No. 2011R10076), Natural Science Foundation of Zhejiang Province, China (No. Y4080342, LY13B010004), and SRF for ROCS, SEM.

Appendix A. Supplementary material

CCDC 876705 and 936230 contains the supplementary crystallographic data for **1** and **2**. These data can be obtained free of charge from The Cambridge Crystallographic Data Centre via www.ccdc.cam.ac.uk/data_request/cif. Supplementary data associated with this article can be found, in the online version, at <http://dx.doi.org/10.1016/j.ica.2014.01.007>.

References

- [1] (a) S. Khatua, J. Kang, J.O. Huh, C.S. Hong, D.G. Churchill, *Cryst. Growth Des.* 10 (2010) 327; (b) L.H. Abdel-Rahman, R.M. El-Khatib, L.A.E. Nassr, A.M. Abu-Dief, *J. Mol. Struct.* 1040 (2013) 9; (c) Z.Z. Li, L. Du, J. Zhou, M.R. Zhu, F.H. Qian, J. Liu, P. Chen, Q.H. Zhao, *Dalton Trans.* 41 (2012) 14397; (d) Y.N. Belokon, V.I. Maleev, D.A. Kataev, T.F. Saveleva, T.V. Skrupskaya, Y.V. Nelyubina, M. North, *Tetrahedron Asymmetry* 20 (2009) 1746; (e) Y.N. Belokon, V.I. Maleev, D.A. Kataev, I.L. Mal'fanov, A.G. Bulychev, M.A. Moskalenko, T.Y.F. Saveleva, T.Y.V. Skrupskaya, K.A. Lyssenko, I.A. Godovikov, M. North, *Tetrahedron Asymmetry* 19 (2008) 822; (f) J. Müller, G. Kehr, R. Fröhlich, G. Erker, *Eur. J. Inorg. Chem.* (2005) 2836.
- [2] (a) C.T. Chen, Y.H. Lin, T.S. Kuo, *J. Am. Chem. Soc.* 130 (2008) 12842; (b) M. Gharagozlou, D.M. Boghaei, *Spectrochim. Acta, Part A: Mol. Biomol. Spectrosc.* 71 (2008) 1617; (c) M. Ebel, D. Rehder, *Inorg. Chem.* 45 (2006) 7083; (d) J.M. Rivera, H. Reyes, A. Cortés, R. Santillan, P.G. Lacroix, C. Lepetit, K. Nakatani, N. Farfán, *Chem. Mater.* 18 (2006) 1174; (e) P.A.N. Reddy, M. Nethaji, A.R. Chakravarty, *Eur. J. Inorg. Chem.* (2004) 1440.
- [3] (a) G. Desiraju, *Acc. Chem. Res.* 24 (1991) 290; (b) K.A. Siddiqui, G.K. Mehrotra, J. Mrozinski, R.J. Butcher, *J. Mol. Struct.* 964 (2010) 18; (c) T. Fujimura, H. Seino, M. Hidai, Y. Mizobe, *J. Organomet. Chem.* 689 (2004)

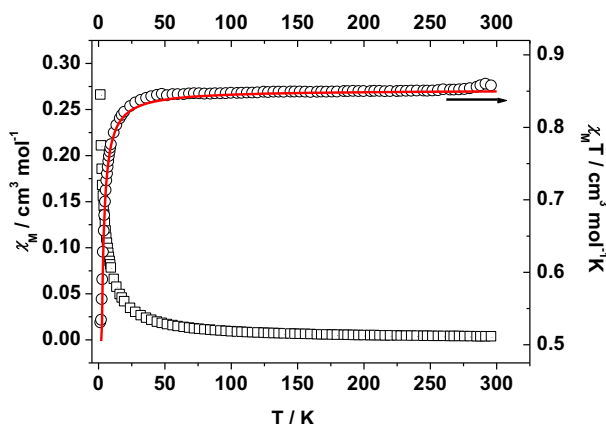


Fig. 5. Temperature dependence of $\chi_M T$ (○) and χ_M (□) for **1**. The solid line corresponds to the best fit according to the parameters in Eq. (1) given in the text.

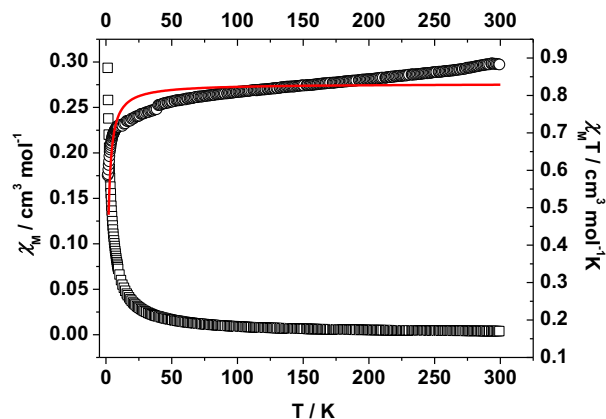


Fig. 6. Temperature dependence of $\chi_M T$ (○) and χ_M (□) for **2**. The solid line corresponds to the best fit according to the parameters in Eq. (1) given in the text.

- 738;
(d) J.K. Bera, T.T. Vo, R.A. Walton, K.R. Dunbar, *Polyhedron* 22 (2003) 3009.
- [4] (a) A. García-Raso, J.J. Fiol, A. López-Zafra, A. Tasada, I. Mata, E. Espinosa, E. Molins, *Polyhedron* 25 (2006) 2295;
(b) A. García-Raso, J.J. Fiol, F. Bádenas, M. Quirós, *Polyhedron* 15 (1996) 4407.
- [5] (a) S. Khatua, K. Kim, J. Kang, J.O. Huh, C.S. Hong, D.G. Churchill, *Eur. J. Inorg. Chem.* (2009) 3266;
(b) B. Lou, F. Jiang, D. Yuan, B. Wu, M. Hong, *Eur. J. Inorg. Chem.* (2005) 3214;
(c) S. Warda, P. Dahlke, S. Wocadlo, W. Massa, C. Friebel, *Inorg. Chim. Acta* 268 (1998) 117;
(d) S.A. Warda, *Acta Crystallogr., Sect. C* 53 (1997) 697.
- [6] (a) H.D. Bian, X.E. Yang, Q. Yu, Z.L. Chen, H. Liang, S.P. Yan, D.Z. Liao, *J. Mol. Struct.* 872 (2008) 40;
(b) S.P. Xu, L. Shi, Y. Pei, Y. Yang, G. Xu, H.L. Zhu, *J. Coord. Chem.* 63 (2010) 3463;
(c) J. Sivy, V. Kettmann, J. Krätsmar-Smogrovic, O. Svajlenova, C. Friebel, *G. Plesch, Z. Anorg. Allg. Chem.* 583 (1990) 55.
- [7] (a) H. Bian, F. Huang, X. Yang, Q. Yu, H. Liang, *J. Coord. Chem.* 61 (2008) 802;
(b) Y.Z. Yuan, J. Zhou, D.Q. Li, X. Liu, Z.F. Chen, K.B. Yu, *Acta Crystallogr., Sect. E: Struct. Rep. Online* 61 (2005) m1444.
- [8] S.Y. New, Y. Thio, L.L. Koh, T.S. Andy Hor, F. Xue, *CrystEngComm* 13 (2011) 2114.
- [9] S.P.S. Rao, H. Manohar, R. Bau, *J. Chem. Soc., Dalton Trans.* (1985) 2051.
- [10] T. Ueki, T. Ashida, Y. Sasada, M. Kakudo, *Acta Crystallogr.* 22 (1967) 870.
- [11] I. Bkouche-Waksmam, J.M. Barbe, A. Kvick, *Acta Crystallogr., Sect. B* 44 (1988) 595.
- [12] T. Ueki, T. Ashida, Y. Sasada, M. Kakudo, *Acta Crystallogr., Sect. B* 25 (1969) 328.
- [13] D.M. Boghaei, M. Gharagozlou, *Spectrochim. Acta, Part A: Mol. Biomol. Spectrosc.* 67 (2007) 944.
- [14] J.F. Cutfield, D. Hall, T.N. Waters, *Chem. Commun.* (1967) 785.
- [15] J.E. Davies, *Acta Crystallogr., Sect. C* 40 (1984) 903.
- [16] X. Zhang, C. Du, D. Chen, M. Huang, *Chin. J. Inorg. Chem.* 26 (2010) 489.
- [17] N. Kobakhidze, N. Farfán, M. Romero, J.M. Méndez-Stivalet, M.G. Ballinas-López, H. García-Ortega, O. Domínguez, R. Santillan, F. Sánchez-Bartéz, I. Gracia-Mora, *J. Organomet. Chem.* 695 (2010) 1189.
- [18] A.R. Minter, A.A. Fuller, A.K. Mapp, *J. Am. Chem. Soc.* 125 (2003) 6846.
- [19] (a) J. Dong, L. Li, G. Liu, T. Xu, D. Wang, *J. Mol. Struct.* 986 (2011) 57;
(b) M.Z. Wang, Z.X. Meng, B.L. Liu, G.L. Cai, C.L. Zhang, X.Y. Wang, *Inorg. Chem. Commun.* 8 (2005) 368;
(c) P.A.N. Reddy, M. Nethaji, A.R. Chakravarty, *Inorg. Chim. Acta* 337 (2002) 450;
(d) G. Plesch, C. Friebel, S.A. Warda, *Transition Met. Chem.* 22 (1997) 433.
- [20] G.L. Qiu, Y.J. Li, W. Yang, Y. Zou, *J. Chem. Crystallogr.* 41 (2011) 898.
- [21] (a) G.M. Sheldrick, *SADABS*, University of Göttingen:Göttingen, Germany, 1996.;
(b) SIR97 program, A. Altomare, M.C. Burla, M. Camalli, G.L. Casciarano, C. Giacovazzo, A. Guagliardi, A.G.G. Moliterni, G. Polidori, R. Spagna, *J. Appl. Cryst.* 32 (1999) 115.
- [22] *SHELXTL* program G.M. Sheldrick, *Acta Crystallogr., Sect. A* 64 (2008) 112.
- [23] (a) G. Marin, V. Kravtsov, Y.A. Simonov, V. Tudor, J. Lipkowski, M. Andruh, *J. Mol. Struct.* 796 (2006) 123;
(b) J. Geng, T. Tao, K.H. Gu, G. Wang, W. Huang, *Inorg. Chem. Commun.* 14 (2011) 1978;
(c) Z.H. Weng, Z.L. Chen, F.P. Liang, *J. Coord. Chem.* 62 (2009) 1801.
- [24] T. Ueki, T. Ashida, V. Sasada, K. Kakudo, *Acta Crystallogr., Sect. B* 25 (1969) 328.
- [25] W.J. Zhou, Y.Z. Jiang, Y. Zou, *Acta Crystallogr., Sect. E* 66 (2010) m579.
- [26] N. Mondal, D.K. Dey, S. Mitra, K.M. Abdul Malik, *Polyhedron* 19 (2000) 2707.
- [27] B. Bleaney, K.D. Bowers, *Proc. R. Soc. London A* 214 (1952) 451.
- [28] P.S. Mukherjee, S. Dalai, G. Mostafa, T.H. Lu, E. Rentschler, N.R. Chaudhuri, *New J. Chem.* 25 (2001) 1203.